Chemical Science

ROYAL SOCIETY OF CHEMISTRY

EDGE ARTICLE

View Article Online
View Journal | View Issue

Cite this: *Chem. Sci.*, 2024, **15**, 20346

All publication charges for this article have been paid for by the Royal Society of Chemistry

Site-selective decarbonylative [4 + 2] annulation of carboxylic acids with terminal alkynes by C–C/C–H activation strategy and cluster catalysis†

Mengjie Cen,[ab] Xinyue Ma,[a] Xi Yang,[a] Shangshang Zhang,[a] Long Liu,[a] Michal Szostak *[c] and Tieqiao Chen *[a]

Cycloaddition and annulation strategies are among the most powerful methods for creating molecular complexity in organic molecules. In this manuscript, we report a highly site-selective palladium-catalyzed decarbonylative [4 + 2] cyclization of carboxylic acids with terminal alkynes by a sequential C–C/C–H bond activation. Most notably, this method represents the first use of carboxylic acids as the ubiquitous and underdeveloped synthons for intramolecular cycloadditions by decarbonylative C–C bond cleavage. The method provides a solution to the long-standing challenge of the regioselective synthesis of substituted naphthalenes by cycloaddition. Mechanistic studies show that this reaction occurs through a sequential process involving the formation of key palladacycle by a sequential C–C/C–H bond activation and highly regioselective alkyne insertion enabled by cluster catalysis. Wide substrate scope for both carboxylic acids and terminal alkynes is demonstrated with high functional group tolerance. Moreover, this reaction is scalable and applicable to the synthesis of functionalized molecules featuring bioactive fragments. This reaction advances the toolbox of redox-neutral carboxylic acid interconversion to cycloaddition processes. We anticipate that this approach will find broad application in organic synthesis, drug discovery and functionalized material research fields.

Received 13th August 2024
Accepted 11th November 2024

DOI: 10.1039/d4sc05429f

rsc.li/chemical-science

Introduction

Cycloaddition and annulation strategies are among the most powerful methods in organic synthesis and an area of intense interest from academic and industrial perspectives.[1,2] In particular, [4 + 2] cycloadditions, such as the venerable Diels–Alder reaction, are of major importance in organic synthesis, drug discovery and functional material science. Catalytic cycloadditions involving regioselective activation of inert bonds are of particular value since they provide nonclassical methods for the creation of molecular complexity by cycloaddition processes. In this context, the naphthalene ring represents a prevalent structural motif found in a plethora of drugs, natural products and advanced materials. Naphthalenes show unique optoelectronic properties and thus are widely used as optical and electronic materials.[3] Over the years, the efficient construction of rings has received significant attention.[4–7] Although straightforward and atom-economic methods for the synthesis of naphthalenes have been established, at present, there are major challenges in deploying this method for the site-selective synthesis of the naphthalene ring. In general, acid-catalyzed electrophilic cyclizations are limited by the site-selectivity at the original aryl ring and restricted to electron-rich arenes.[5] In contrast, the transition-metal-catalyzed approach is one of the most straightforward methods for the construction of carbocycles; however, in the case of naphthalene rings, this approach is limited to symmetrical coupling partners to avoid regio-selectivity issues at the newly formed benzene ring and only limited functional groups can be introduced by this process.[6] Furthermore, the method since intramolecular cyclization approach does not represent an efficient the preparation of functionalized substrates is a major limitation.[7] Thus, despite their significant utility, general and modular methods for the synthesis of polyfunctionalized naphthalene rings with high site-specificity of the introduction of various functional groups from the readily available starting materials are underdeveloped.

Carboxylic acids are among the most ubiquitous, naturally abundant and commercially available substrates in organic synthesis.[8] Recent years have witnessed an explosion of interest in the utilization of the carboxylic acid functional group by metal catalysis to facilitate the synthesis of functionalized molecules.[9–12] Thus far, carboxylic acids have been widely used

[a]School of Chemistry and Chemical Engineering, Hainan University, Haikou, 570228, China. E-mail: chentieqiao@hnu.edu.cn

[b]Hainan Research Academy of Environmental Sciences, Haikou, 571127, PR China

[c]Department of Chemistry, Rutgers University, 73 Warren Street, Newark, NJ 07102, USA. E-mail: michal.szostak@rutgers.edu

† Electronic supplementary information (ESI) available. CCDC 2311101. For ESI and crystallographic data in CIF or other electronic format see DOI: https://doi.org/10.1039/d4sc05429f

as the acyl source in organic synthesis after the selective oxidative addition of the acyl bond to transition metals.[10] Significant advances have also been made in the cross-coupling of carboxylic acids by orthogonal activation pathways by decarboxylation[11] and decarbonylation.[12] However, the use of carboxylic acids as modular synthons for intermolecular site-selective cycloadditions to rapidly build-up molecular complexity is underdeveloped, despite their untapped utility as broadly available precursors for this class of transformations.

Herein, we report a highly site-selective palladium-catalyzed decarbonylative [4 + 2] cyclization of carboxylic acids with terminal alkynes by a sequential C–C/C–H bond activation. Most notably, this method represents the first use of carboxylic acids as the ubiquitous and underdeveloped synthons for intramolecular cycloadditions by decarbonylative C–C bond cleavage. The method provides a solution to the long-standing challenge of the regioselective synthesis of substituted naphthalenes by cycloaddition. Mechanistic studies show that this reaction occurs through a sequential process involving the formation of key palladacycle by a sequential C–C/C–H bond activation and highly regioselective alkyne insertion enabled by cluster catalysis. Wide substrate scope for both carboxylic acids and terminal alkynes is demonstrated with high functional group tolerance (>60 examples) (Scheme 1).

Valuable functional group, such as ethers, thioethers, halides, fluorinated functional groups, esters, ketones, aldehydes, nitriles, various heterocycles, silicon protecting groups, alkenes and even organoboranes are well tolerated under the reaction conditions. Moreover, this reaction is scalable and applicable to the smooth synthesis of functionalized molecules featuring bioactive fragments. This reaction advances the toolbox of redox-neutral carboxylic acid interconversion to cycloaddition processes and enables the site-selective synthesis of functionalized naphthalenes from readily available carboxylic acids. We anticipate that this approach will find broad application in organic synthesis, drug discovery and functionalized material research fields.

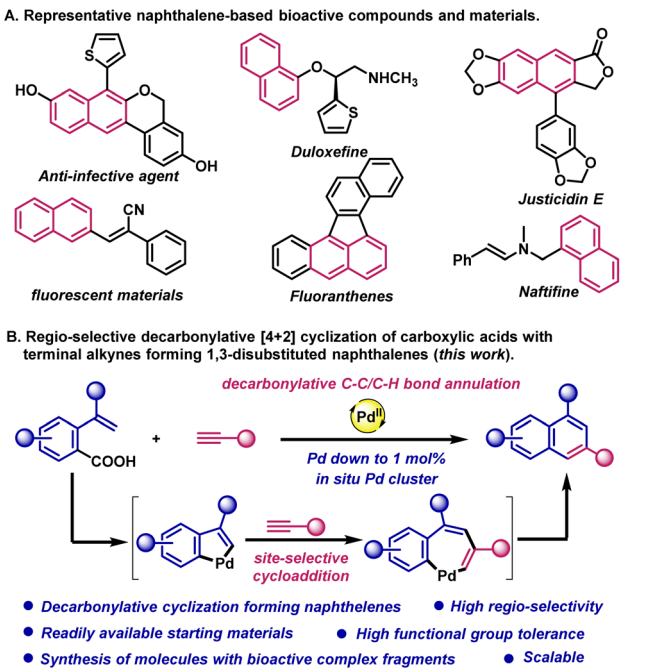

Scheme 1 (A) Representative naphthalene-based bioactive natural products and materials. (B) Decarbonylative site-selective C–C/C–H cycloaddition of carboxylic acids forming functionalized naphthalenes.

Results and discussion

Reaction optimization

We initiated our investigation by examining the cycloaddition of 2-(1-phenylvinyl)benzoic acid **1a** and phenylacetylene **2a** as a model system as summarized in Table 1. We are delighted to find that reacting the mixture of **1a** (0.2 mmol), **2a** (0.4 mmol), $PdCl_2$ (5 mol%), TFP (10 mol%), Piv_2O (1.4 equiv.), DMAP (4-dimethylaminopyridine, 1.0 equiv.) and LiBr (0.5 equiv.) in dioxane at 160 °C for 12 h, affords the cyclization product **3a** with full site-specificity in 84% yield (Table 1, entry 1). Control reactions demonstrate that palladium catalyst, anhydride

Table 1 Reaction. Optimization[a]

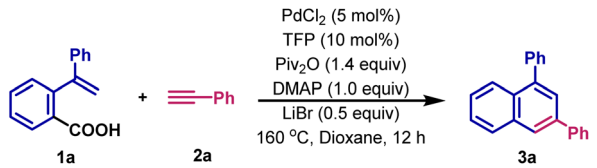

Entry	Variation from the standard conditions	Yield[b] of **3a** (%)
1	None	84
2	Without Pd catalyst	N.D.
3	Without anhydride Piv_2O	N.D.
4	Without base DMAP	Trace
5	$Pd(acac)_2$ or $Pd(OAc)_2$ instead of $PdCl_2$	70/42
6	$Pd2(dba)_3$ instead of $PdCl_2$	50
6	$NiCl_2$ instead of $PdC1_2$	Trace
7	Boc_2O, Ac_20 instead of Piv_2O	29/56
9	Pyridine, Et_3N or DBU instead of DMAP	Trace/12/43
10	Without LiBr	34
11	LiF, LiCl and $LiFePO_4$ instead of LiBr	41/70/75
12	NaBr and KBr instead of LiBr	35/55
13	Without phosphine ligand	63
14	Xantphos and DPE-phos instead of TFP	73/68
15	$(4\text{-F-Ph})_3P$ and $(4\text{-Me-Ph})_3P$ instead of TFP	67/64
16	THF, DME and DEE instead of dioxane	49/50/52
17	Toluene and hexane instead of dioxane	53/52

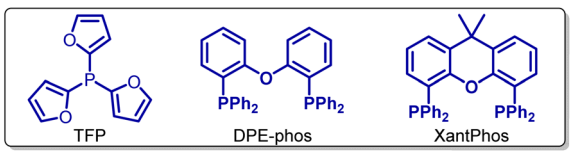

[a] Reaction conditions: 2-(1-phenylvinyl)benzoic acid **1a** (0.2 mmol), phenylacetylene **2a** (0.4 mmol, 2.0 equiv. based on **1a**), cat. [Pd] (5 mol%), ligand (10 mol%), anhydride (1.4 equiv.), DMAP (1.0 equiv.), solvent (2.0 mL), N_2, 160 °C, 12 h. [b] GC yield using dodecane as an internal standard.

Table 2 Substrate scope of carboxylic acids and terminal alkynes[a]

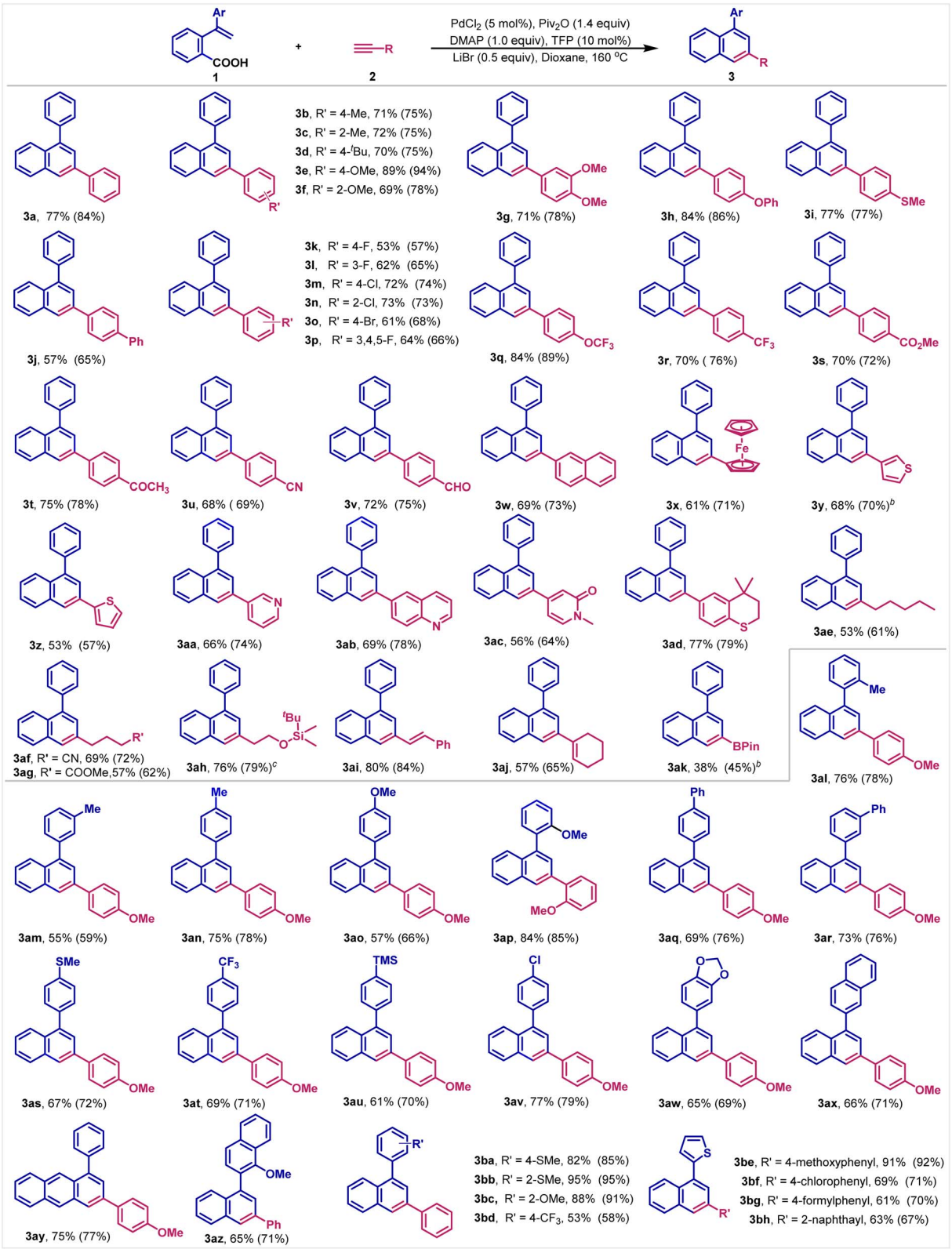

[a] Reaction conditions: carboxylic acid **1** (0.2 mmol), terminal alkyne **2** (0.4 mmol, 2.0 equiv.), $PdCl_2$ (5 mol%), TFP (10 mol%), Piv_2O (0.28 mmol, 1.4 equiv.), dioxane (2.0 mL), N_2, 160 °C, 12 h. Isolated yield. GC yield is shown in parentheses. [b] Terminal alkyne **2** (4.0 equiv.) is used. [c] LiI instead of LiBr.

activator and base are essential to this reaction, with no or only a trace amount of **3a** being detected in their absence (Table 1, entries 2–4). Other Pd(II) catalysts, such as $Pd(acac)_2$ or $Pd(OAc)_2$, can also promote the reaction (Table 1, entry 5). Pd(0) catalysts, such as $Pd_2(dba)_3$, affords **3a** in 50% yield under similar reaction conditions (Table 1, entry 6). Interestingly, $NiCl_2$ is also a capable catalyst, providing a promising lead for future studies (Table 1, entry 7). Furthermore, when Boc_2O and Ac_2O are used instead of Piv_2O as the activating reagent, the yield of **3a** decreases (Table 1, entry 8). The yield is also lower when pyridine, Et_3N or DBU are used instead of DMAP (Table 1, entry 9). The results might be ascribed to their weak nucleophilicity.[13] Interestingly, LiBr plays an important role in this reaction;[14] with only 34% yield of **3a** being observed in its absence (Table 1, entry 10). LiF, LiCl and $LiFePO_4$ can also serve as promoters, but their efficiency is lower (Table 1, entry 11). Furthermore, we established that KBr has a positive effect, but NaBr is ineffective (Table 1, entries 12). Next, we extensively investigated the phosphine ligand. In its absence, only 63% yield of **3a** is obtained (Table 1, entry 13). Bidentate Xantphos and DPE-phos show good catalytic efficiency (Table 1, entry 14), while monodentate phosphines, such as $(4\text{-F-Ph})_3P$ and $(4\text{-Me-Ph})_3P$ also afford lower yields (Table 1, entries 14 and 15). Importantly, the reaction can take place in several ether solvents such as THF, DME and DEE (Table 1, entry 16), while toluene and hexane also afford similar yields (Table 1, entry 17). It should be noted that the reaction shows excellent regioselectivity; the byproduct 1,4-disubstituted naphthalene is not detected in the crude reaction mixtures by GC-MS. Additional optimization details are included in the ESI.†

Scope studies

With the optimal reaction conditions in hand, the substrate scope for both carboxylic acids and terminal alkynes was then investigated. Importantly, we establish that the reaction shows excellent generality with respect to both reaction components. In terms of alkynes, both aromatic and aliphatic terminal alkynes including those with various functional groups work well under the reaction conditions. After isolation and purification, **3a** is obtained in 77% yield. Substrates with electron-donating groups, such as alkyl (–Me, –^{t}Bu), alkoxy (–OMe, –OPh), thiomethyl (–SMe) and phenyl (–Ph) at the benzene ring are readily converted into the corresponding naphthalenes in 57–89% yields (Table 2, **3b–3j**). Halogen groups (F, Cl and Br) survive well to furnish the halogenated products in 53–73% yields (Table 2, **3k–3p**). These products provide functional handles that can be easily further functionalized by traditional cross-coupling reactions, demonstrating orthogonality of the carboxylic acid electrophile. Likewise, high yields are also obtained from substrates containing a range of electron-withdrawing groups, such as OCF_3, CF_3, ester, acetyl, CN or formyl at the benzene ring (Table 2, **3q–3v**). To our delight, the π-extended terminal alkynes, such as 2-ethynylnaphthalene and ethylnylferrocene can produce the cyclized products in good yields (Table 2, **3w–3x**). It is further worth noting that chelating heterocycles that can coordinate with transition-metals are compatible under the reaction conditions, including thiophenes (Table 2, **3y–3z**), pyridine (Table 2, **3aa**), quinoline (Table 2, **3ab**), *N*-methyl-2-pyridinone (Table 2, **3ac**) and thiochromane (Table 2, **3ad**), all of these substrates are smoothly transformed into the corresponding cyclizing products in good to high yields, furnishing π-conjugates naphthalene products that are relevant in the synthesis of advanced materials.

Furthermore, we are pleased to learn that in addition to aromatic terminal alkynes, aliphatic alkynes are also applicable to this reaction and afford the corresponding products with full site-selectivity. For example, 1-heptyne reacts well with **1a** to give the desired 3-alkyl-naphthalene (Table 2, **3ae**). Alkynes decorated with cyano, ester and siloxy groups prove to be effective substrates (Table 2, **3af–3ah**). It is worth noting that alkenyl double bonds are well-tolerated under the reaction conditions (Table 2, **3ai** and **3aj**). Furthermore, the reaction enables to introduce even an organoboronic ester into the naphthalene framework, demonstrating the functional group orthogonality of the carboxylic acid decarbonylative annulation approach (Table 2, **3ak**). However, ethyl propiolate and ethoxyethyne did not work under the reaction conditions. The results might be ascribed to their low boiling points. Internal alkynes like diphenylacetylene and prop-1-yn-1-ylbenzene were not suitable to this reaction either, since the corresponding products were only detected in less than 10% yields.

With respect to the carboxylic acid component, the reaction also shows high functional group tolerance. Thus, alkyl, methoxy, phenyl, methylthio, trimethylsilyl, chloro and trifluoromethyl groups are well-tolerated under the reaction conditions (Table 2, **3al–3av**). To our delight, large conjugated π-systems can be efficiently constructed by the strategy as exemplified by the anthracenyl and binaphthyl rings (Table 2, **3aw–3az**). These products have found wide applications in photo-material chemistry. Finally, selectivity studies with different terminal alkynes and carboxylic acids are conducted, affording the corresponding naphthalenes in 53–95% yields with full site-selectivity, further demonstrating the generality of this new reaction (Table 2, **3ba–3bh**).

Synthesis of molecules bearing bioactive fragment

We demonstrate that this novel method enables facile introduction of bioactive molecular fragments into the naphthalene skeleton. For example, naphthalene with an antioxidant flavone fragment is generated in 72% yield under the standard reaction conditions (Scheme 2b, **3bi**). The molecular structure is determined by X-ray analysis (CCDC number: 2311101), unambiguously confirming the site-selectivity of the cycloaddition. By the strategy, estrone, isoeugenol, flavone, zingiberone and perillaldehyde fragments are also smoothly introduced (Scheme 2b, **3bj–3bm**), demonstrating the potential of this new method in medicinal chemistry and natural products campaigns.

Scale-up

To further evaluate the practicality of this new method, a scale-up reaction was conducted. As shown in Scheme 2a, when the reaction of **1a** and **2a** is performed on a 1 mmol scale, **3a** is

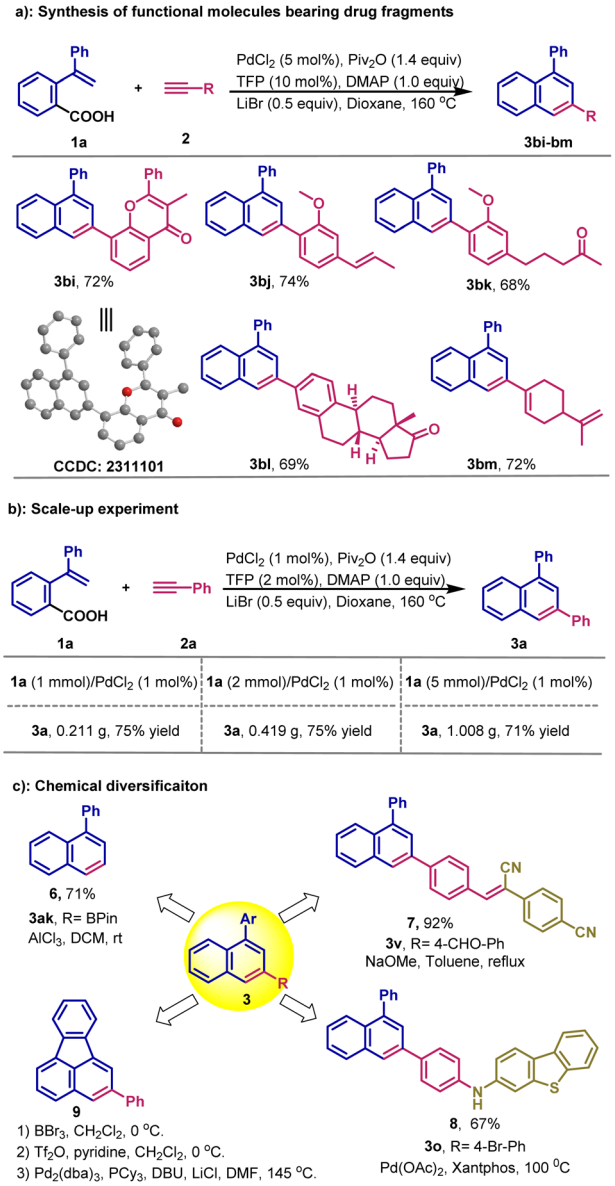

Scheme 2 Synthetic applications. (a) Scale-up experiments. (b) Synthesis of functional molecules bearing drug fragments. (c) Chemical diversification.

produced in 75% yield (0.211 g). High yields are also obtained at 2 mmol and 5 mmol scales. It should be noted that only 1 mol% $PdCl_2$ is required in these reactions, demonstrating efficiency of the decarbonylative process.

Chemical diversification

As demonstrated by the scope studies, we find that this novel reaction tolerates a variety of electrophilic groups, which could facilitate further derivatization to synthesize target functional molecules not easily available by other methods (Scheme 2c). For example, we show that **3ak** can readily undergo protodeborylation to produce the corresponding 1-substituted naphthalene **6**. Furthermore, product **3v** with a formyl group readily reacts with benzeneacetonitrile to afford the fluorescent photochromic **7**, which exhibits distinct light-triggered changes in the emission colors.[15] Similarly, product **3o** with a Br substituent can produce the diarylamine product **8** through a conventional Buchwald–Hartwig cross-coupling. It is worth noting is that compound **8** is a structural segment of organic electroluminescent devices.[16] Furthermore, dibenzofluoranthenes, such as **9**, can be readily synthesized from product **3ap**.[17] These results highlight the practical value of this new site-selective decarbonylative cycloaddition of carboxylic acids in organic synthesis.

Mechanistic studies

To gain mechanistic insight into the reaction, control experiments are performed (Scheme 3). First, to probe the selectivity of this reaction, intermolecular competition experiments are conducted. When 4-trifluoromethyl phenyl acetylene **2r** and 4-methoxyl phenyl acetylene **2e** react with carboxylic acid **1a**, the

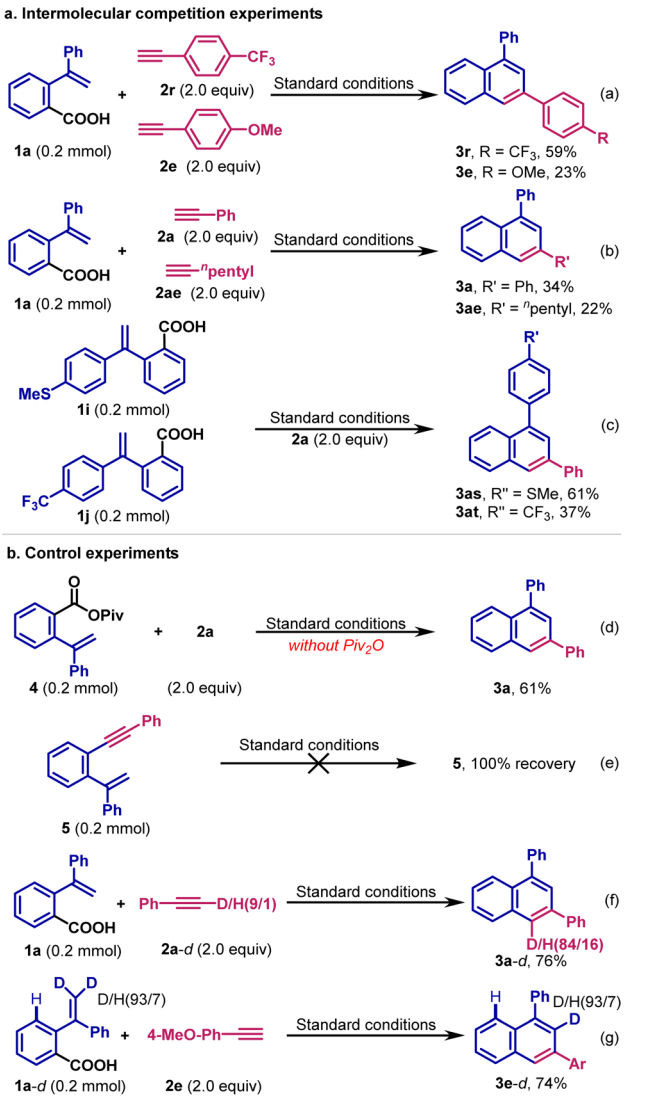

Scheme 3 Competition experiments, control experiments and deuterium experiments.

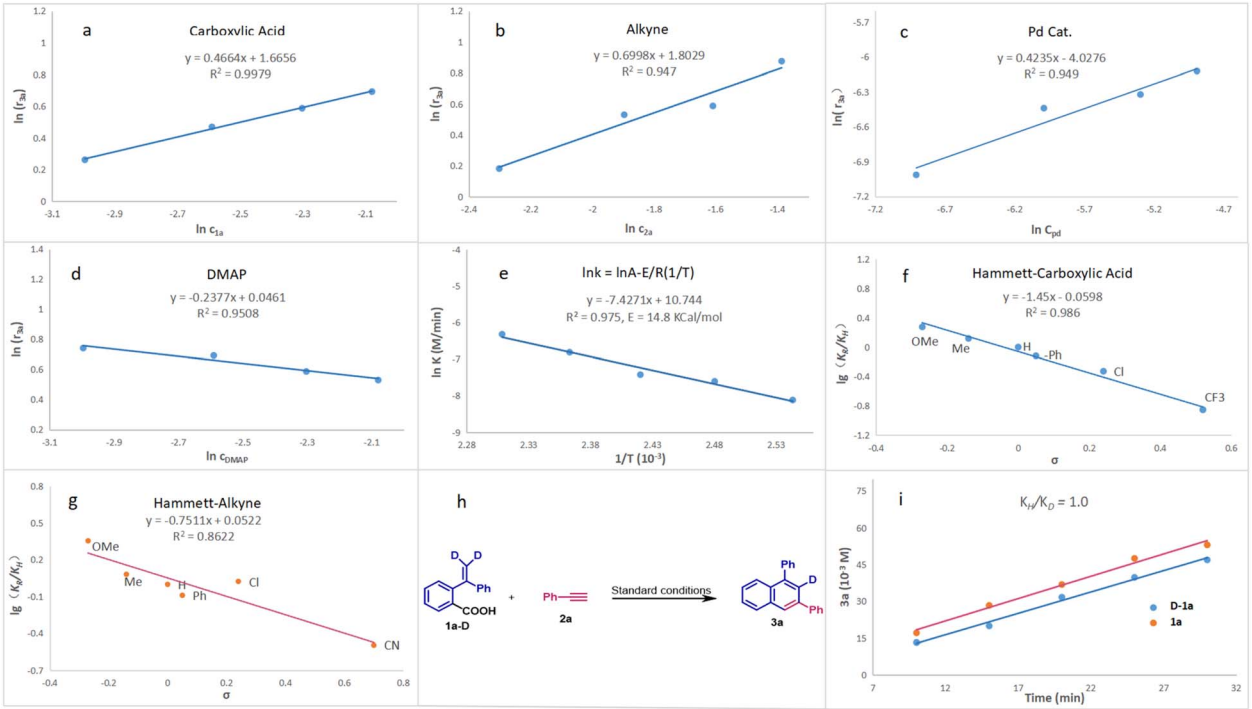

Fig. 1 Kinetic analysis, Hammett analysis and KIE experiments. (a) Carboxylic acid *vs.* initial rate. (b) Alkyne *vs.* initial rate. (c) Pd-cat *vs.* initial rate. (d) DMAP *vs.* initial rate. (e) Arrhenius plots: plot of ln *k vs.* 1/*T*. (f) *para*-Substituted carboxylic acids with alkyne. (g) *para*-Substituted alkynes with carboxylic acid. (h and i) Kinetic isotopic effects (KIE).

corresponding products **3r** and **3e** are produced in 59% and 23% yields, respectively (Scheme 3a). When phenylacetylene **2a** is allowed to compete with hept-1-yne **2ae**, **3a** is obtained in 34% yield, and **3ae** is generated in 22% yield (Scheme 3b). These results indicate that the reaction favors electron-deficient terminal alkynes. Furthermore, when phenylacetylene **2a** is reacted with carboxylic acids **1i** and **1j**, the product **3as** is produced in 61% yield, and **3at** in 37% yield, indicating that electron-rich carboxylic acids are favored (Scheme 3c).

Next, we hypothesize that carboxylic acid is firstly activated *in situ* to produce the active mixed anhydride. Indeed, we have synthesized the mixed anhydride **4** and allowed it to react with phenyl acetylene **2a**, resulting in 65% yield of **3a** under similar reaction conditions (Scheme 3d). During the reaction of **1a** with **2a**, the *ipso*-decarbonylative product **5** is detected by GC-MS. To probe the role of **5** as the intermediate, which could undergo intramolecular cyclization to produce the target product, we synthesized **5** and subjected it to the reaction conditions (Scheme 3e). However, we find that **3a** is not generated and **5** is quantitatively recovered. When carboxylic acid **1a** reacts with deuterated **2a**-*d*, **3a**-*d* is produced in 76% yield with 84% deuterium incorporation at the 4-position (Scheme 3f). We also synthesized deuterated carboxylic acid **1a**-*d*, and reacted it with 4-methoxyl phenyl acetylene **2e** to produce **3e**-*d* in 74% yield under the reaction conditions (Scheme 3g). In compound **3e**-*d*, the C2-position is fully deuterated, while no deuterium is detected at the C4-position. These results indicate that **5** is not the intermediate of this decarbonylative cycloaddition. Furthermore, the *ortho*-vinyl group remained intact during the reaction, while the decrease of deuterium incorporation at the C4-position in **3a**-*d* could be ascribed to the hydrogen–deuterium exchange of terminal alkyne under the reaction conditions.

Kinetic studies

The kinetic analysis was subsequently conducted (Fig. 1). We find that the reaction shows half-order dependence on carboxylic acid and Pd-catalyst. For terminal alkynes and DMAP, the rate is 0.7-order and zero-order, respectively (Fig. 1a–d). The activation energy is also calculated based on the reaction temperature and the value is 14.8 kcal mol^{-1}. Since the reaction is performed at 160 °C, the intrinsic activation energy would usually be more than 30 kcal mol^{-1}. This suggests that the reaction might be mediated by palladium clusters, leading to a difference by diffusion. To validate this hypothesis, the mercury poisoning experiments are conducted (Scheme 4a). We find that mercury can inhibit the reaction; in particular, when 100 equiv. mercury (calculated on the basis of palladium) is used, the reaction is almost completely inhibited. These results show that the reaction involves a heterogeneous process.[18] Moreover, we analyzed the reaction mixture by MALDI-TOF MS and found some fragments such Pd2, Pd4 and Pd5, further supporting the formation of palladium clusters. Subsequently, we investigated the effect of ligand's loading. It is found that the yield of **3a** decreased as the increase of phosphine TFP's loading (Scheme 4b). Worth noting is that the selectivity also decreased. Under the standard reaction conditions, the isomer **3a′** and the

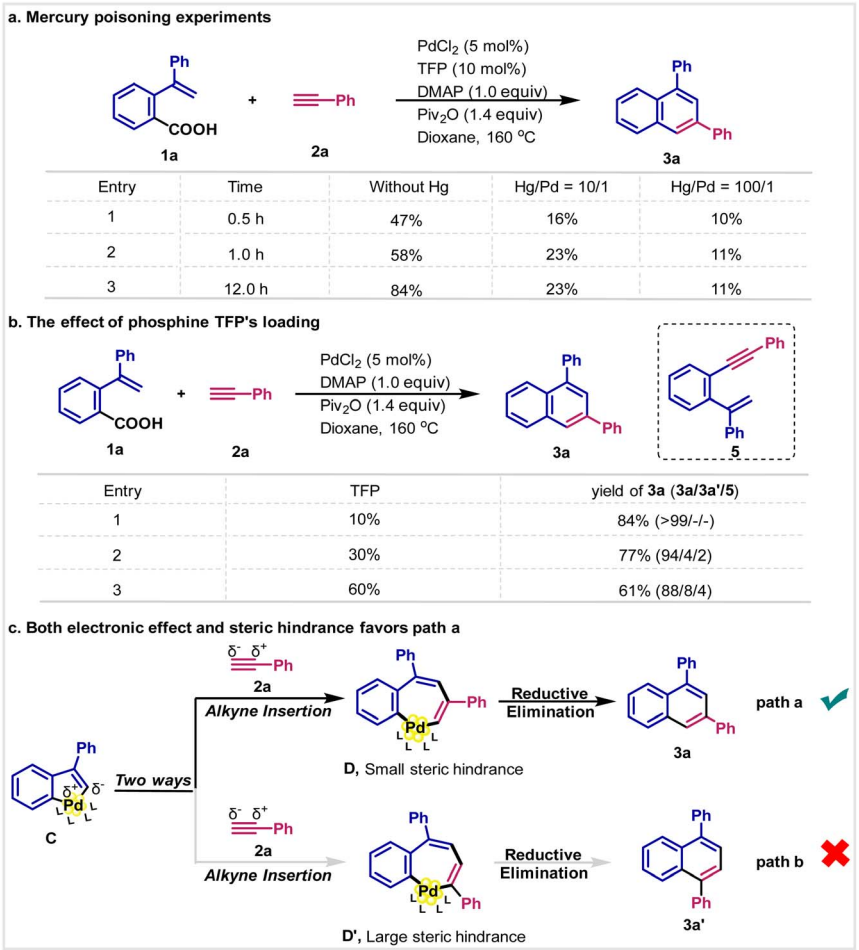

Scheme 4 The investigation of reaction selectivity.

ipso-coupling product **5** almost could not be detected by GC-MS, while both **3a**′ and **5** were generated when more TFP was added. It is known that ligand would stabilize the molecular palladium complexes, stopping the formation of palladium cluster. Thus, those results might be ascribed to the delayed formation of Pd cluster.[19]

As described below, complex **C** would be the key intermediate in this reaction (Scheme 4c). Considering from the steric hindrance, compared with C_{aryl}–Pd bond, it would be easier for terminal alkynes to insert into C_{vinyl}–Pd bond. In addition, both electronic and steric factors would favor path a to give isomer **3a**. In this reaction, the steric hindrance is further increased due to the formation of palladium clusters, thus very high selectivity to **3a** is observed. Finally, we performed Hammett analysis (Fig. 1f–h). A negative slope ($\rho = -1.45$) is observed for the reaction of *para*-substituted carboxylic acids **1** with phenylacetylene **2a** (Fig. 1f). A comparatively smaller value ($\rho = -0.75$) is found for the reaction of *para*-substituted phenylacetylenes **2** with carboxylic acid **1a** (Fig. 1g). These results indicate that the reaction is more affected by the electronic properties of the carboxylic acid. Furthermore, kinetic isotope experiments (KIE) of **2a**-*d* with **3a** are performed (Fig. 1h). A small kinetic isotope effect ($k_H/k_D = 1.0$) is obtained, indicating that the C–H cleavage is not the rate-determining step in this reaction.

Proposed mechanism

On the basis of mechanistic studies, a plausible mechanism involving palladacycle formation by a sequential C–C/C–H activation and a subsequent regioselective insertion of terminal alkynes is proposed (Scheme 5). As shown in Scheme 5, carboxylic acid **1a** is firstly activated by anhydride Piv_2O to produce the mixed anhydride **4**. Then, the acyl C–O bond oxidatively adds to the active Pd(0) catalyst generated *in situ* to afford **A**. This acyl–Pd intermediate undergoes decarbonylation and vinnyl C–H cleavage by the assistance of $PivO^-$ anion forming the five-membered palladacycle **C**.[20] The subsequent insertion of terminal alkyne proceeds with exquisite regioselectivity to generate the seven-membered arylpalladium **D**. Finally, reductive elimination of **D** produces the target product **3** and regenerates the active Pd(0) catalyst.[21] The byproduct **6** obtained from intermediate **A** through intramolecular C–H activative cyclization can be observed by GC-MS. It should be noted that fragment of intermediates **B**, **C** and **D** have been detected by MALDI-TOF MS (see ESI†), further supporting the proposed decarbonylative C–C/C–H catalytic cycle. It should be mentioned that the detected fragment of intermediates **B**, **C** and **D** did not contain phosphine ligand. The result might be

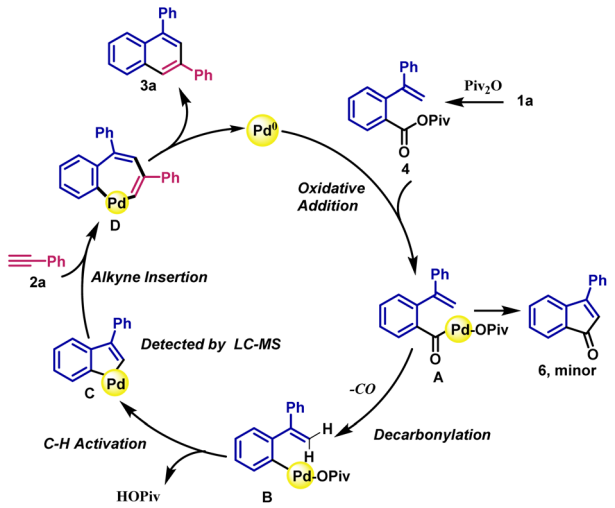

Scheme 5 Proposed mechanism. For clarity, the ligand is omitted.

ascribed to the relatively weak coordination between Pd and phosphine ligand as well as the weak Pd–Pd bonds in cluster.

In conclusion, we have disclosed an exquisitely site-selective decarbonylative cycloaddition of carboxylic acids with terminal alkynes by sequential C–C/C–H bond activation. Most notably, this method represents the first use of carboxylic acids as the ubiquitous and underdeveloped synthons for intramolecular cycloadditions by decarbonylative C–C bond cleavage. Furthermore, the method provides a solution to the challenge of the regioselective synthesis of substituted naphthalenes by cycloaddition. Wide substrate scope for both carboxylic acids and terminal alkynes is demonstrated with excellent functional group tolerance. In addition, the reaction utility is demonstrated in the construction of complex molecules bearing bioactive fragments and product derivatization through readily tolerated active groups. Extensive mechanistic studies show this reaction takes place through formation of a key five-membered palladacycle and regioselective transfer insertion of terminal alkynes determining the high regioselectivity of this process by the formation of palladium clusters. This reaction advances the toolbox of redox-neutral carboxylic acid interconversion to cycloaddition processes. This reactivity platform is likely to find wide application in organic synthesis, drug discovery and functional material research fields.

Data availability

The ESI† includes all experimental details, including optimization of the synthetic method, synthesis and characterization of all starting materials and products reported in this study, and mechanistic studies. NMR spectra of all products reported are included as well.

Author contributions

M. C. performed the experiments. M. S. and T. C. conceived the project and wrote the manuscript. X. M., X. Y., S. Z. and L. L. provided crucial suggestions to the main concept of the project and revised the manuscript.

Conflicts of interest

There are no conflicts to declare.

Acknowledgements

T. C. thanks the National Nature and Science Foundation of China (Grant No. 21871070, 22261015) and the Key R&D project of Hainan province (No. ZDYF2020168, XTCX2022STA01). M. S. thanks Rutgers University and the NSF (CAREER CHE-1650766) for financial support.

Notes and references

1 Selected reviews, see: (*a*) D. Mal and P. Pahari, *Chem. Rev.*, 2007, **107**, 1892–1918; (*b*) F. Gallier, A. Martel and G. Dujardin, *Angew. Chem., Int. Ed.*, 2017, **56**, 12424–12458; (*c*) L. Chen, K. Chen and S. Zhu, *Chem*, 2018, **4**, 1208–1262; (*d*) N. Wang, Z. Wu, J. Wang, N. Ullah and Y. Lu, *Chem. Soc. Rev.*, 2021, **50**, 9766–9793; (*e*) M. Zhang, B. Qu, B. Shi, W. Xiao and L. Lu, *Chem. Soc. Rev.*, 2022, **51**, 4146–4174.

2 Selected examples, see: (*a*) L. Jiao, S. Ye and Z. Yu, *J. Am. Chem. Soc.*, 2008, **130**, 7178–7179; (*b*) X. Li, W. Song and W. Tang, *J. Am. Chem. Soc.*, 2013, **135**, 16797–16800; (*c*) S. Banerjee, S. Sathyamoorthi, J. D. Boisa and R. N. Zare, *Chem. Sci.*, 2017, **8**, 7003–7008; (*d*) Y. Wang, W. Liao, Y. Wang, L. Jiao and Z. Yu, *J. Am. Chem. Soc.*, 2022, **144**, 2624–2636; (*e*) M. Sindlinger, M. Ströbele, J. Grunenberg and H. F. Bettinger, *Chem. Sci.*, 2023, **14**, 10478–10487; (*f*) Y. Ding, J. Wu and H. Huang, *J. Am. Chem. Soc.*, 2023, **145**, 4982–4988; (*g*) D. Svatunek, A. Murnauer, Z. Tan, K. N. Houk and K. Lang, *Chem. Sci.*, 2024, **15**, 2229–2235.

3 Selected reviews, see: (*a*) J. E. Anthony, *Chem. Rev.*, 2006, **106**, 5028–5048; (*b*) Q. Ye and C. Chi, *Chem. Mater.*, 2014, **26**, 4046–4056; (*c*) M. Stępien, E. Gonka, M. Zyla and N. Sprutta, *Chem. Rev.*, 2017, **117**, 3479–3716.

4 Selected reviews, see: (*a*) C. K. Bradsher, *Chem. Rev.*, 1987, **87**, 1277–1297; (*b*) S. Saito and Y. Yamamoto, *Chem. Rev.*, 2000, **100**, 2901–2915; (*c*) E. Aguilar, R. Sanz, M. A. Fernandez-Rodr and P. García-García, *Chem. Rev.*, 2016, **116**, 8256–8311.

5 Selected examples, see: (*a*) N. Asao, T. Nogami, S. Lee and Y. Yamamoto, *J. Am. Chem. Soc.*, 2003, **125**, 10921–10925; (*b*) N. Asao, T. Nogami, S. Lee and Y. Yamamoto, *J. Am. Chem. Soc.*, 2004, **126**, 7458–7459; (*c*) A. Matsumoto, L. Ilies and E. Nakamura, *J. Am. Chem. Soc.*, 2011, **133**, 6557–6559; (*d*) Y. Li, A. Yagiab and K. Itami, *Chem. Sci.*, 2019, **10**, 5470–5475.

6 Selected examples, see: (*a*) Q. Huang and C. R. Larock, *Org. Lett.*, 2002, **4**, 2505–2508; (*b*) M. V. Pham and N. Cramer, *Angew. Chem., Int. Ed.*, 2014, **53**, 3484–3487; (*c*) A. Seoane, C. Comanescu, N. Casanova, R. García-Fandiño, X. Diz, J. L. Mascarenas and M. Gulías, *Angew. Chem., Int. Ed.*, 2019, **58**, 1700–1704; (*d*) A. Wu, H. Qian, W. Zhao and J. Sun, *Chem. Sci.*, 2020, **11**, 7957–7962; (*e*) J. Guo, Y. Liu, X. Lin, T. Tang, B. Wang, P. Hu, K. Zhao, F. Song and Z. Shi, *Angew. Chem., Int. Ed.*, 2021, **60**, 19079–19084.

7 Selected examples on the intramolecular annulation, see: (*a*) K. Maeyama and N. Iwasawa, *J. Am. Chem. Soc.*, 1998, **120**,

1928–1929; (*b*) R. K. Mohamed, S. Mondal, B. Gold, C. J. Evoniuk, T. Banerjee, K. Hanson and I. V. Alabugin, *J. Am. Chem. Soc.*, 2015, **137**, 6335–6349; (*c*) M. Schukin, T. Wurm, J. Bucher, M. C. Dietl, C. J. Aschendorf, M. Rudolph, F. Rominger, J. Graf and A. S. K. Hashmi, *ACS Catal.*, 2024, **14**, 2107–2114.

8 (*a*) G.-I. Badea and G. L. Radu, *Carboxylic Acid-Key Role in Life Sciences*, InTech, 2018; (*b*) C. Lamberth and J. Dinges, *Bioactive Carboxylic Compound Classes: Pharmaceuticals and Agrochemicals*, Wiley-VCH, Weinheim, Germany, 2016; (*c*) C. Ballatore, D. M. Huryn and A. B. Smith III, *ChemMedChem*, 2013, **8**, 385–395; (*d*) S. B. Beil, T. Q. Chen, N. E. Intermaggio and D. W. C. MacMillan, *Acc. Chem. Res.*, 2022, **55**, 3481–3494; (*e*) D. Seidel and C. Min, *Chem. Soc. Rev.*, 2017, **46**, 5889–5902.

9 Selected reviews, see: (*a*) N. Rodriguez and L. J. Gooßen, *Chem. Soc. Rev.*, 2011, **40**, 5030–5048; (*b*) Y. Wei, P. Hu, M. Zhang and W. Su, *Chem. Rev.*, 2017, **117**, 8864–8907; (*c*) A. Varenikov, E. Shapiro and M. Gandelman, *Chem. Rev.*, 2021, **121**, 412–484; (*d*) D. M. Kitcatt, S. Nicolle and A. Lee, *Chem. Soc. Rev.*, 2022, **51**, 1415–1453.

10 Selected examples, see: (*a*) C. Zhao, X. Jia and X. Wang, *J. Am. Chem. Soc.*, 2014, **136**, 17645–17651; (*b*) R. Ruzi, K. Liu, C. Zhu and J. Xie, *Nat. Commun.*, 2020, **11**, 3312–3321; (*c*) X. Jiang, F. Sheng, Y. Zhang, G. Deng and S. Zhu, *J. Am. Chem. Soc.*, 2022, **144**, 21448–21456; (*d*) X. Liu, X. Li, L. Liu, T. Huang, W. Chen, M. Szostak and T. Chen, *ACS Catal.*, 2023, **13**, 5819–5827.

11 Selected examples, see: (*a*) A. G. Myers, D. Tanaka and M. R. Mannion, *J. Am. Chem. Soc.*, 2002, **124**, 11250–11521; (*b*) L. J. Goossen, G. Deng and L. M. Levy, *Science*, 2006, **313**, 662–664; (*c*) L. Candish, M. Freitag, T. Gensch and F. Glorius, *Chem. Sci.*, 2017, **8**, 3618–3622; (*d*) C. Li, J. Wang, L. M. Barton, S. Yu, M. Tian, D. S. Peters, M. Kumar, A. W. Yu, K. A. Johnson, A. K. Chatterjee, M. Yan and P. S. Baran, *Science*, 2017, **356**, eaam7355; (*e*) J. T. Edwards, R. R. Merchant, K. S. Mcclymont, K. W. Knouse, T. Qin, L. R. Malins, B. Vokits, S. A. Shaw, D.-H. Bao, F.-L. Wei, T. Zhou, M. D. Eastgate and P. S. Baran, *Nature*, 2017, **545**, 213–218; (*f*) V. T. Nguyen, G. C. Haug, D. Nguyen, N. T. H. Vuong, H. D. Armana and O. V. Larionov, *Chem. Sci.*, 2021, **12**, 6429–6436; (*g*) K. P. Lee, J. L. Harper, T. H. Kim, H. C. Noh, D. Kim, P. H. Cheong and P. Lee, *Chem. Sci.*, 2023, **14**, 643–649; (*h*) Y. Hioki, M. Costantini, J. Griffin, K. C. Harper, M. P. B. Merini, Y. Nissl and P. S. Kawamata, *Science*, 2023, **380**, 81–87; (*i*) D. L. Lipilin, M. O. Zubkov, M. D. Kosobokov and A. D. Dilman, *Chem. Sci.*, 2024, **15**, 644–650.

12 Selected examples, see: (*a*) F. Pan, Z. Lei, H. Wang, H. Li, J. Sun and Z. Shi, *Angew. Chem., Int. Ed.*, 2013, **52**, 2063–2067; (*b*) A. Chatterjee and V. R. Jensen, *ACS Catal.*, 2017, **7**, 2543–2547; (*c*) C. Liu, C. Ji, X. Hong and X. M. Szostak, *Angew. Chem., Int. Ed.*, 2018, **57**, 16721–16726; (*d*) C. Liu, Z. Pin, C. Ji, X. Hong and M. Szostak, *Chem. Sci.*, 2019, **10**, 5736–5742; (*e*) C. A. Malapit, J. R. Bour, S. R. Laursen and M. S. Sanford, *J. Am. Chem. Soc.*, 2019, **141**, 17322–17330; (*f*) C. Liu, C. Ji, T. Zhou, X. Hong and M. Szostak, *Angew. Chem., Int. Ed.*, 2021, **60**, 10690–10699; (*g*) X. Deng, J. Guo, X. Zhang, X. Wang and W. Su, *Angew. Chem., Int. Ed.*, 2021, **60**, 24510–24518; (*h*) K. Xiang, S. Zhang, L. Liu and T. Q. Chen, *Org. Chem. Front.*, 2021, **8**, 2543–2550.

13 D. Chen, L. Xu, Y. Yu, Q. Mo, X. Qi and C. Liu, *Angew. Chem., Int. Ed.*, 2023, **62**, e202215168.

14 Z. Wang, Z. Zhang and X. Lu, *Organometallics*, 2000, **19**, 775–780.

15 N. F. Konig, D. Mutruc and S. Hecht, *J. Am. Chem. Soc.*, 2021, **143**, 9162–9168.

16 R. Usman, A. Khan, M. Wang, Y. Luo, W. Sun, H. Sun, C. Du and N. He, *Cryst. Growth Des.*, 2018, **18**, 6001–6008.

17 S. Fatayer, N. B. Poddar, S. Quiroga, F. Schulz, B. Schuler, S. V. Kalpathy, G. Meyer, D. Perez, E. Guitian, D. Pena, M. J. Wornat and L. Gross, *J. Am. Chem. Soc.*, 2018, **140**, 8156–8161.

18 (*a*) D. Pun, T. Diao and S. S. Stahl, *J. Am. Chem. Soc.*, 2013, **135**, 8213–8221; (*b*) V. M. Chernyshev, A. V. Astakhov, I. E. Chikunov, R. V. Tyurin, D. B. Eremin, G. S. Ranny, V. N. Khrustalev and V. P. Ananikov, *ACS Catal.*, 2019, **9**, 2984–2995; (*c*) X. Li, S. Mitchell, Y. Fang, J. Li, J. Perez-Ramirez and J. Lu, *Nat. Rev. Chem*, 2023, **7**, 754–767; (*d*) N. T. S. Phan, M. V. D. Sluys and C. W. Jones, *Adv. Synth. Catal.*, 2006, **348**, 609–679; (*e*) O. N. Gorunova, I. M. Novitskiy, Y. K. Grishin, I. P. Gloriozov, V. A. Roznyatovsky, V. N. Khrustalev, K. A. Kochetkov and V. V. Dunina, *Organometallics*, 2018, **17**, 2842–2858.

19 It is reported that clusters show excellent catalytic activity and selectivity, see: (*a*) R. A. T. M. van Benthem, H. Hiemstra, P. W. N. M. van Leeuwen, J. W. Geus and W. N. Speckamp, *Angew Chem. Int. Ed. Engl.*, 1995, **34**, 457–460; (*b*) D. D. Tang, K. D. Collins and F. Glorius, *J. Am. Chem. Soc.*, 2013, **135**, 7450–7453; (*c*) K. D. Collins, R. Honeker, S. Vasquez-Cespedes, D. D. Tang and F. Glorius, *Chem. Sci.*, 2015, **6**, 1816–1824; (*d*) M. Li, Y. Yang, A. A. Rafi, M. Oschmann, E. S. Grape, A. K. Inge, A. Cordova and J. B. Backvall, *Angew. Chem., Int. Ed.*, 2020, **59**, 10391–10395; (*e*) M. Li and J. Backvall, *Acc. Chem. Res.*, 2021, **54**, 2275–2286; (*f*) J. Yao, Z. Zhang and Z. Li, *J. Am. Chem. Soc.*, 2024, **146**, 8839–8846.

20 Selected examples, see: (*a*) R. Giri, X. Chen and J. Yu, *Angew. Chem., Int. Ed.*, 2005, **44**, 2112–2115; (*b*) R. Giri, J. Liang, J. Lei, J. Li, D. Wang, X. Chen, I. C. Naggar, C. Guo, B. M. Foxman and J. Yu, *Angew. Chem., Int. Ed.*, 2005, **44**, 7420–7424; (*c*) S. I. Gorelsky, D. Lapointe and K. Fagnou, *J. Am. Chem. Soc.*, 2008, **130**, 10848–10849; (*d*) Q. He and N. Chatani, *Angew. Chem., Int. Ed.*, 2021, **60**, 5189–5192; (*e*) M. Wheatley, M. Zuccarello, M. Tsitopoulou, S. A. Macgregor and O. Baudoin, *ACS Catal.*, 2023, **13**, 12563–12570.

21 (*a*) V. G. Landge, J. M. Maxwell, P. Chand-Thakuri, M. Kapoor, E. T. Diemler, E. T. Diemler and M. C. Young, *JACS Au*, 2021, **1**, 13–21; (*b*) V. G. Landge, A. Mishra, W. Thotamune, A. L. Bonds, I. Alahakoon, A. Karunarathne and M. C. Young, *Chem Catal.*, 2023, **3**, 100809–100824. According to the two refereces, the mechanism through alkene insertion can not be excluded completely at present.